Arabian Journal for Science and Engineering (2022) 47:5167–5186
https://doi.org/10.1007/s13369-021-06423-8

RESEARCH ARTICLE-CIVIL ENGINEERING

Laboratory Study and Statistical Analysis on the Hydraulic Failure of Sandy Soils

Shayan Ghasemian Langroudi[1] · Ali M. Rajabi[2] · Amirali Zad[1] · Tohid Mahdavi[1]

Received: 26 May 2021 / Accepted: 18 November 2021 / Published online: 27 January 2022

Abstract

The sand boiling phenomenon occurs downstream of hydraulic structures, and the continuation of this phenomenon could lead to a structural failure. In this paper, by developing a device to simulate sand boiling, experimental tests have been performed to determine the critical hydraulic gradient on various sandy soil. The effect of different parameters was evaluated such as four relative densities (0, 20, 50 and 80%), uniformity coefficient, woven and non-woven geotextiles in both single and double-layer states and the particle size distribution. Based on the results, with increasing the relative density and uniformity coefficient, the sand resistance against the hydraulic failure improved and also in soils with $C_u = 1$, coarser sands have indicated more resistance to the boiling. In improvement by geotextile, reinforced sands beard more water load than natural sands, and the type and layer number of reinforcements have affected the test results. In addition, a statistical comparison has been performed between the experimental results and the proposed equation by Terzaghi to calculate the critical hydraulic gradient. Finally, by using experimental results, a linear and nonlinear regression model is presented to predict the required seepage force for the hydraulic failure of the specimens.

Keywords Hydraulic failure · Sand boiling · Critical hydraulic gradient · Uniformity coefficient · Seepage force · And geotextile

List of Symbols

γ_{dmax}	Maximum dry unit weight (g/cm^3)
γ_{dmin}	Minimum dry unit weight (g/cm^3)
γ_w	Unit weight of water (g/cm^3)
ΔH	Difference head (m)
A	Sample cross section (cm^2)
C_c	Curvature coefficient (dimensionless)
C_u	Uniformity coefficient (dimensionless)
D_{10}	Effective particles size (mm)
D_{50}	Mean particles size (mm)
D_r	Relative density (dimensionless)
F	Seepage force (N)
G_s	Specific gravity of natural soil (dimensionless)
H_1	Upstream head (m)
H_2	Downstream head (m)
i_{cr}	Critical hydraulic gradient (dimensionless)
K	Permeability coefficient (cm/s)
MQ	Model quality (dimensionless)
Q	Discharge flow (cm^3/s)
R^2	Determination coefficient
Re	Reynolds number (dimensionless)
RMSE	Root-mean-squared error
v	Flow velocity (cm/s)
V	Sample volume (cm^3)
W	Weight of the sample (g)
β_i	Constant coefficient of the hypothesize function (dimensionless)

✉ Amirali Zad
a.zad@iauctb.ac.ir

Shayan Ghasemian Langroudi
Shayanghasemian3@gmail.com

Ali M. Rajabi
amrajabi@ut.ac.ir; amrajabi@ymail.com

Tohid Mahdavi
Toh.mahdavi.eng@iauctb.ac.ir

[1] Department of Civil Engineering, Central Tehran Branch, Islamic Azad University, Tehran, Iran

[2] Engineering Geology Department, School of Geology, College of Science, University of Tehran, Tehran, Iran

1 Introduction

Hydraulic structures such as dams, water canals, and embankments are important structures that are built along rivers to supply, store, and transfer water for urban, industrial and agricultural use. The occurrence of hydraulic failures such as the rapid drawdown in the upstream, sand boiling, piping in the downstream and uplift (inside the body and foundation of a dam) can be considered as hazards for these structures. The spread of these events leads to the fraction of the water structures and can result in major Life and financial losses.

The German BAW Code [1] defines hydraulic failure in four modes including uplift, internal erosion, heave, and piping.

Uplift failure occurs when the pore water pressure under the soil layers with very low permeability overcomes the weight of the soil structure and moves the structure upward in an integrated way. Lateral and uplift forces due to groundwater flow can adversely affect the stability of structures such as dams and weirs [2].

Internal erosion of soil as a type of hydraulic failure refers to the process whereby fine particles are detached from a soil structure to the liquid stream flowing through the soil pores and subsequently migrate with the liquid phase [3]. Internal erosion can lead to the piping phenomenon and consequently the failure of levees and dams [4].

Heave is another type of hydraulic failure that causes boiling of the sand particles. Jewel et al. [5] performed a sand boiling test on silica sand and reported that the cause of sand boiling is zero shear stress of cohesionless soils and concluded that there is a linear relationship between critical shear stress and hydraulic gradients and evaluated the trend of shear stress variations as a decrease in upward seepage. Sand boiling can be considered as a kind of damage due to liquefaction [6].

Piping, as one of the critical patterns of internal erosion, has been reported as a major cause for failures of embankment dams and levees [7]. In this phenomenon like sand boiling, the erosive force of the seepage by overcoming the shear stress of the soil causes the separation of particles from each other and the creation of flow channels. Backward erosion piping occurs when non-plastic soil particles are removed at a seepage exit point [8]. Richards and Reddy [9] introduced three modes for piping behavior in hydraulic structures including backward erosion, erosion due to concentrated seepage and suffusion. The Teton Dam in 1976 was one of the hydraulic structures that collapsed by the piping phenomenon in the dam abutment and caused huge damages [10].

According to theoretical studies, sand boiling and piping occur when the amount of hydraulic gradient exceeds the critical hydraulic gradient (i_{cr}) of the soil and the soil does not show resistance to water seepage. Terzaghi [11], Wu [12], Liu [13], and Zhou et al. [14] presented theoretical equations to predict i_{cr}. The basis of these relations is the zero value of effective stress and the force equilibrium for a particle of soil. The presented relationship by Terzaghi [11] to determine the i_{cr} is:

$$i_{\mathrm{cr}} = \frac{G_{\mathrm{s}} - 1}{e + 1} \tag{1}$$

According to Eq. (1), soil compaction (void ratio and porosity) is an important and effective factor in the calculation of i_{cr}.

Furumoto et al. [15], Sivakumar & Vasudevan [16], Das et al. [17], Das and Viswanadham [18], Estabragh et al. [19], Estabragh et al. [20], Yang and Wang [21], Yang et al. [22], and Langroudi et al. [23] measured the required hydraulic gradients for the hydraulic failure of natural and fiber-reinforced samples by fabricating a device to create upward water seepage. In these studies, the fibers were randomly distributed in the soil and increasing the percentage and length of the fibers, increased the i_{cr} of the samples. Also, in the researches of Sivakumar & Vasudevan [16] and Estabragh et al. [20] for the experimental results, a regression model (linear and quadratic) has been presented that predicts the correlation between seepage velocity and seepage force with parameters such as fiber length and percentage. These statistical analyses have been performed using errors optimization of theoretical models relative to observational data.

In this study with designing and fabricating a device to create upward seepage (to simulate sand boiling phenomenon), the effect of uniformity coefficient and relative density (D_{r}) on the i_{cr} of the soil was investigated. In addition, the effect of using single and double-layer woven and non-woven geotextiles on the sand hydraulic parameters (permeability coefficient, seepage force and critical hydraulic gradient) have been evaluated. Also, ten completely uniform soil samples (with a coefficient of uniformity equal to 1) with maximum porosity and different particles size (diameter) have been considered to measure the critical hydraulic gradient. In addition to the experimental tests, a statistical comparison has been performed between the test results and the presented relationship by Terzaghi [11] (common and widely used model for determining the critical hydraulic gradient) to determine the certainty of Terzaghi's relationship. Finally, two prediction models of linear and nonlinear have been applied to the experimental results which will predict the values of seepage force related to the sand boiling.

2 Material properties

In this study, to examine the phenomenon of sand boiling, four types of granular soils with $C_u > 1$ and ten types of com-

Table 1 Physical and mechanical properties of soils with $C_u > 1$

Soil type	Soil1	Soil2	Soil3	Soil4
G_s	2.65	2.65	2.65	2.65
D_{50} (mm)	0.36	0.82	0.79	0.77
D_{10} (mm)	0.17	0.27	0.2	0.14
C_c	1.06	1.31	1.45	1.58
C_u	2.02	3.38	4.46	6.21
e_{max}	0.93	0.85	0.81	0.79
e_{min}	0.58	0.47	0.45	0.43
Soil classification	SP	SP	SP	SW

Table 2 Physical and mechanical properties of soils with $C_u = 1$

Soil type	D (mm)	e_{max}	γ dmin (gr/cm3)
Soil5	4.75	0.96	1.36
Soil6	3.35	1.00	1.33
Soil7	2.36	1.06	1.29
Soil8	2	1.05	1.30
Soil9	1.18	1.07	1.28
Soil10	1	1.16	1.23
Soil11	0.600	1.15	1.24
Soil12	0.425	1.14	1.24
Soil13	0.250	1.19	1.21
Soil14	0.180	1.22	1.20

pletely uniform soils with $C_u = 1$ were used. These soils are clean sands that were extracted from the Firoozkooh mountain mine (located in the north of Iran) and their constituent minerals are quartz and silica.

2.1 Sandy Soils with $C_u > 1$

Four types of sandy soils with uniformity coefficients of 2.02, 3.38, 4.46, and 6.21 were considered in this study. Based on the sieve analysis test, three of them are classified as SP (poorly graded sand) and the other one graded as well-graded sand according to the Unified classification system (ASTM D2487-17 [24]). Table 1 and Fig. 1 display the physical and mechanical properties and gradation curves for soils 1 to 4, respectively. The maximum and minimum void ratios in this table have been obtained in accordance with the test of minimum and maximum dry densities of granular soil ([25]).

2.2 Sandy Soils with $C_u = 1$

By using sieves No. 4, 6, 8, 10, 16, 18, 30, 40, 60 and 80, uniform soils have been prepared and specific gravity (G_s) for all samples is 2.67. Table 2 demonstrates the physical and mechanical properties of the completely uniform soils used in this study. Based on this table, due to the diameter of the constant particles for each specimen, the values of uniformity and curvature coefficient for soils 5 to 14 become 1.

2.3 Reinforcement Specifications

In this study, two types of geotextile (woven and Non-woven) have been used for soil improvement, which were placed in the soil horizontally. The reinforcements are made of polyester and their main difference between them is in the opening size and the water permeability. Table3 shows the

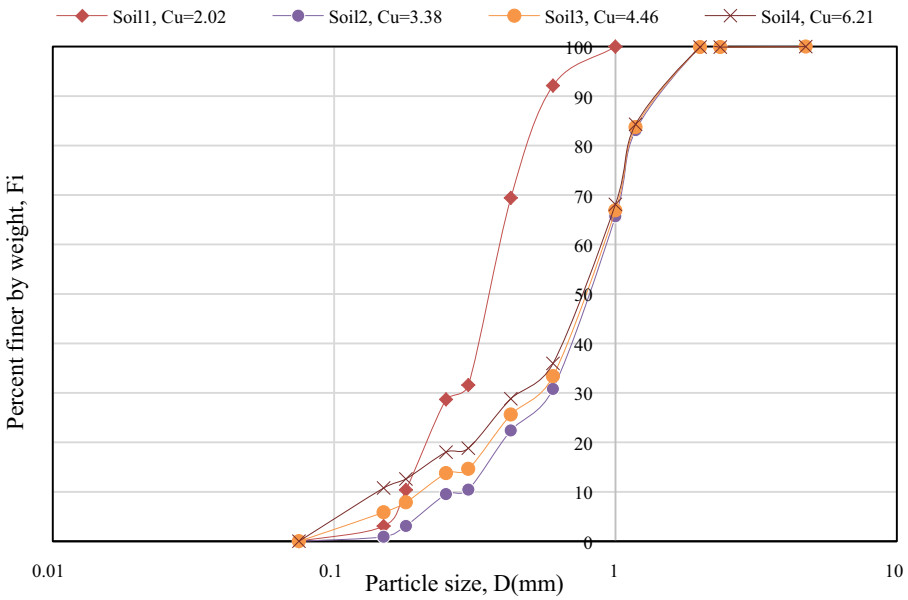

Fig. 1 The grain size distribution of soils ($C_u > 1$)

Table 3 Physical and mechanical properties of geotextiles

Material name	Geotextile type	Permeability (cm/s)	Tensile strength (N)	AOS (mm)	Thickness (mm)
Woven	Polyester	0.01	1250	0.07	Less than 1
Nonwoven	Polyester	0.24	700	0.21	1

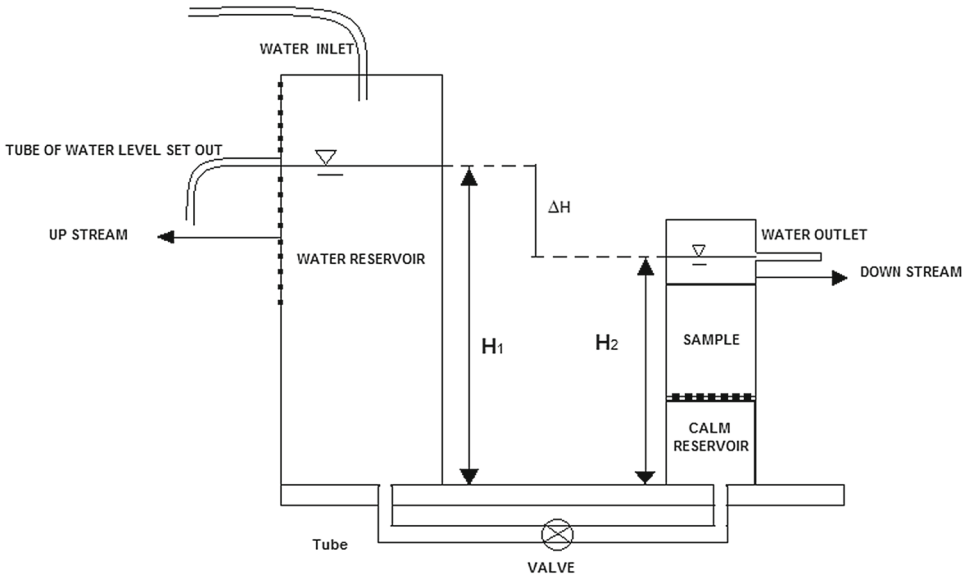

Fig. 2 Schematic design of upward seepage apparatus

physical and mechanical characteristics of woven and nonwoven geotextiles in this research.

3 Sand Boiling Test Device

There is no standard test equipment for determining the resistance of soil against hydraulic failure (i.e. boiling or piping). Skempton & Brogan [26], Fuurmoto et al. [15], Sivakumar & Vasudevan [16], Das et al. [17], Das and Viswanadham [18], Estabragh et al. [19], Estabragh et al. [20], and Yang et al. [22] designed different devices to determine the critical hydraulic gradient by simulating the phenomenon of piping and sand boiling. In this study, considering the sand boiling phenomena, a device has been fabricated. Figures 2 and 3 illustrate the schematic and prototype of the device.

As it can be seen, on the left side of the apparatus, a cylindrical reservoir with an inner diameter of 10 cm and a height of 1 m to supply water was installed. There are some circular holes with a diameter of 8 mm on the wall of the water reservoir that was defined at a distance of 2 cm from each other. These holes adjust the reservoir water level (upstream head). To connect the upstream (left side of the device) to the downstream (right side of the device), a water transfer tube with a diameter of 1 cm has been used. In the path of this tube, a water flow control valve was fabricated to gradually increase the water head of the upstream. On the other side of the water transfer tube, there is a calm reservoir, a sample cell and a downstream ring in the cylindrical form were designed placed on top of each other. The calm reservoir was made of Plexiglass with a diameter and height of 5 and 10 cm, respectively, and the sample cell with a height of 10 cm was placed above it. To observe the flow of water and the boiling phenomenon, the sample cell was considered transparent. For the cell floor, a screen with the number 200($D = 75$ μm) has been used which causes the uniform distribution of water pressure and prevents falling soil particles inside the calm reservoir. The outlet tube has been connected to the downstream transparent ring at a distance of 2 cm over the sample surface that directs the outlet water from the system to the outside to measure the outflow rate. In Fig. 2, H2 and H1 indicate the height of the outlet tube (downstream water head) and the elevation of the water inside the reservoir (upstream water head) versus the desired base level. In this system, the head difference between the upstream and downstream (ΔH) is equal to:

$$\Delta H = H_1 - H_2 \tag{2}$$

Since the height of the sample cell is 10 cm, the amount of applied hydraulic gradient on the specimen is equal to:

$$i = \frac{\Delta H}{(L \cong 10\ \text{cm})} \tag{3}$$

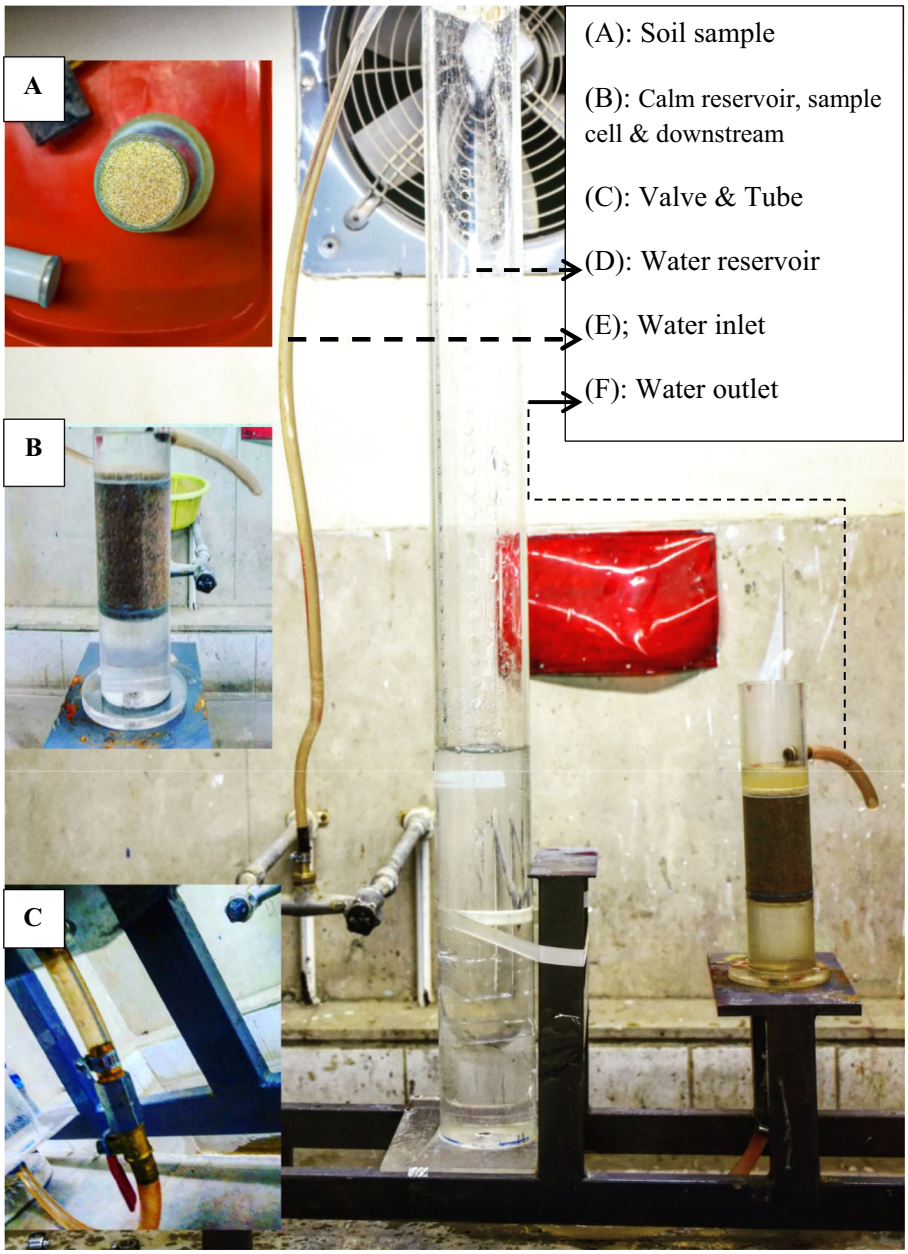

Fig. 3 Overview photo of upward seepage device

4 Sample Preparation and Test Procedure

4.1 Samples Preparation

In this paper, for soils 1 to 4 ($C_u > 1$), four relative densities of 0, 20, 50, and 80% have been considered. For soils 5 to 14 ($C_u = 1$), samples with the loose condition were arranged. To prepare the samples with different compaction conditions, the test of minimum and maximum dry densities of granular soil was performed. To perform this test following the standard (ASTM D4254 and 4253 [27, 28]), the vibration and sand precipitation methods have been used.

Figure 4 depicts the variations of maximum and minimum dry unit weight for sandy soils in terms of the uniformity coefficient. According to this figure, for soils 1 to 4 with $G_s = 2.65$, values of the maximum and minimum dry density increase with increasing uniformity. Indeed, soil porosity at a certain relative density decreases with increasing uniformity coefficient.

Arvelo [29] by performing the modified standard proctor test on sandy soils examined the effect of parameters such as fine percentage (clay and silt) and the uniformity coefficient on the results of compaction tests and found out that the unit weight of the soil increases with increasing the uniformity coefficient of the soil.

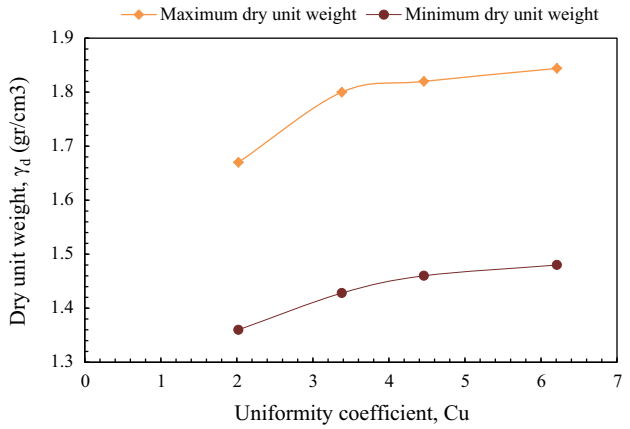

Fig. 4 Variations of maximum and minimum dry unit weight with a uniformity coefficient

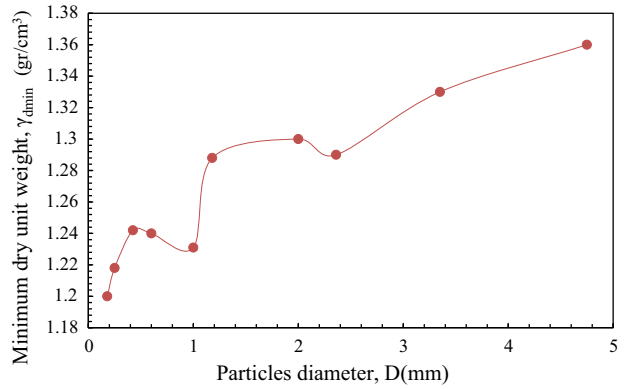

Fig. 5 Variations of minimum dry unit weight against the diameter of the particles ($Cu = 1$)

As mentioned before, for soils 5 to 14 ($C_u = 1$) the sand pluviation technique has been used to make the samples in the loose conditions. Figure 5 displays the variations of minimum dry unit weight in the term of the materials diameters for completely uniform soils. As it can be seen, the minimum dry density rises with an increase in the aggregate diameter. It should be noted that there are exceptions in some points of this diagram. A similar trend for uniform sands has also been reported by Islam et al. [30].

After conducting the relative density tests on the materials, samples 1 to 4 were made at different relative densities. The weight of each sample inside the cell (W) at a certain relative density of D_r is obtained from Eq. (4):

$$W = \frac{\gamma_{dmin}}{1 - \left(\frac{D_r}{\gamma_{dmax}}\right)(\gamma_{dmax} - \gamma_{dmin})} V \quad (4)$$

where V is the sample cell volume. Because of considering the loosest compaction state for soils 5 to 14, the sample weight (W) is calculated using Eq. (5):

$$W = \gamma_{dmin} V \quad (5)$$

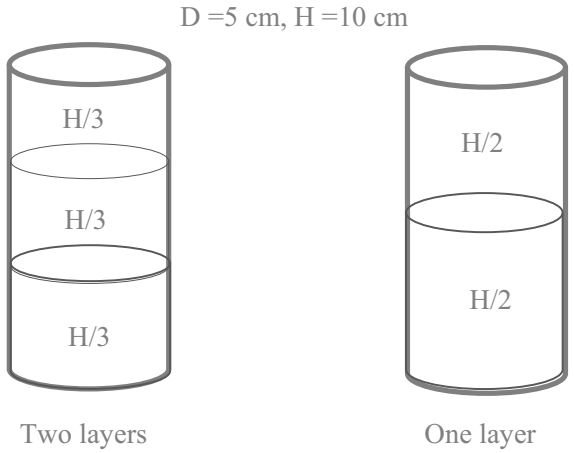

(a)

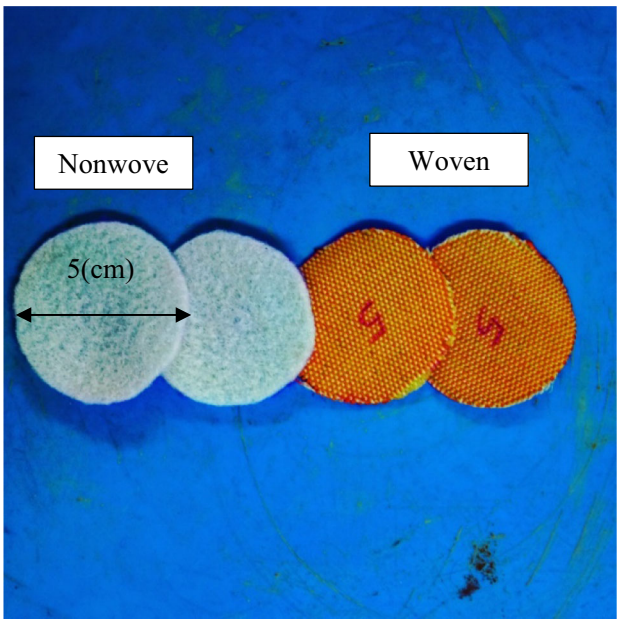

(b)

Fig. 6 **a** Location of the geotextiles layers in the cell of the sand boiling apparatus, **b**: Geotextile texture

For reinforced sand samples with geotextiles, a relative density of 80% was considered. According to Fig. 6(6-a) in reinforced sand with one geotextile layer, the reinforcement element is placed at the center of the apparatus cell. In other words, the position of the reinforcement, in this case, was at a distance of h/2 from the base of the sample cell and in the two-player mode, the distance between the geotextiles was h/3 (h is the height of the cell of the sand boiling device in this study).

4.2 Test Procedure

After preparing the samples at different relative densities, the sample cell is placed on the calm reservoir. Then the water

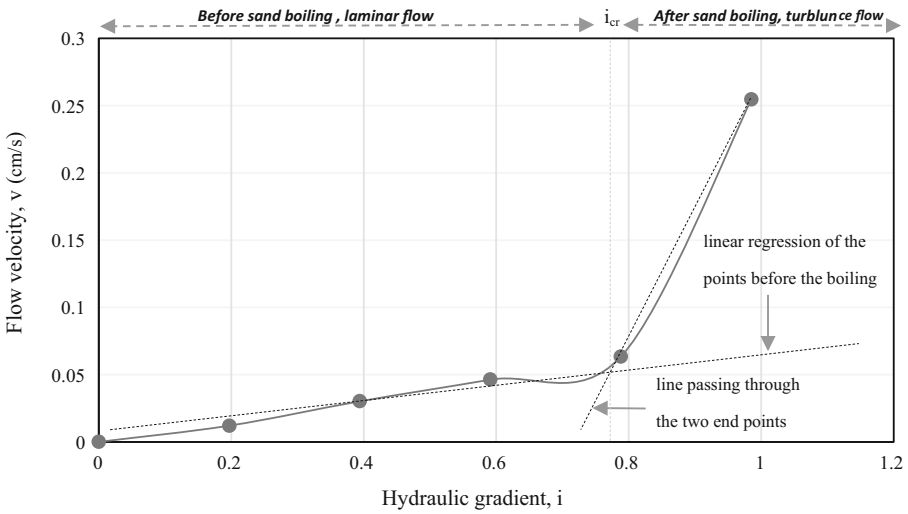

Fig. 7 Diagram of water flow velocity against hydraulic gradient for soil sample 1 ($D_r = 0\%$)

supply pipe is opened to the desired extent so that the water reservoir is filled to a level of 2 cm above the water outlet tube and the excess water of the system is removed through the hole on the wall of the reservoir. In fact, according to the length of 10 cm of the sample, a hydraulic gradient of 0.2 is created between the upstream and downstream of the device. Next by opening the water flow control valve, water enters the calm reservoir and the sample cell through the transfer tube. The flow discharge rate (Q) is calculated by measuring the weight of the outlet water (m) in time of t(s) from Eq. (6).

$$Q = \frac{m}{\gamma_w t} \tag{6}$$

The velocity of water flow into the soil is obtained by having the area of a cross-section perpendicular to the direction of flow (A) (Eq. 7):

$$v = \frac{Q}{A} \tag{7}$$

This step is completed by closing the flow valve. In the following, the height of the reservoir water increases by 2 cm in each stage and, as in the first stage, by measuring the flow rate (Q) for each reservoir water elevation (upstream head), the flow velocity corresponding to the hydraulic gradient is calculated. These steps continue until the occurrence of the sand boiling. Signs such as an increase in discharge, the heave of the sample surface, the muddy water downstream, and the upward movement of grains indicate that the hydraulic failure has occurred and soil can no longer control the downstream flow. Finally, to analyze the obtained results from the sand boiling test, the flow velocity diagram is plotted versus the hydraulic gradient (Fig. 7). Based on this diagram, the hydraulic parameters of the sample such as permeability coefficient (k), critical hydraulic gradient (i_{cr}), and seepage force are determined. In this study by following Darcy's law, to calculate the permeability coefficient of the samples, from the average flow velocity to hydraulic gradient ratios for different points of this graph (v-i). The extracted data belong to points that have a Reynolds number of less than 1 (the laminar flow) [31].

According to Fig. 7, the intersection of the linear regression of the points before the boiling with the line passing through the two endpoints of the experiment shows v_c and i_{cr} (critical flow velocity and hydraulic gradient). By drawing a vertical line at this point of intersection, this chart (v-i) is divided into two parts before and after boiling occurrence. In Fig. 7 using this method, the critical hydraulic gradient of sample 1 with for loose condition is obtained 0.78. By obtaining the i_{cr}, based on Eq. (8), the values of the seepage force for the hydraulic failure of each sample can be calculated.

$$F = i_{cr}\gamma_w V \tag{8}$$

The flow before and after sand boiling illustrate in Fig. 8. Under conditions of $i > i_{cr}$ (after breaking the v-i curve), hydraulic failure occurs for the specimens and with a sudden increase in the flow discharge, the flow mode changes from a laminar flow to turbulence flow downstream and as a result, the water becomes muddy.

5 Results and Discussion

In this research, 40 experimental tests have been performed to measure the hydraulic characteristics of different types of sandy soils (natural and reinforced). Tables 4 and 5 demonstrate the results of sand boiling tests for sandy soils with a uniformity coefficient greater than 1 in the reinforced and unreinforced conditions. Also in Table 6, the results from the hydraulic failure tests of perfectly uniform sands ($C_u = 1$) have been summarized.

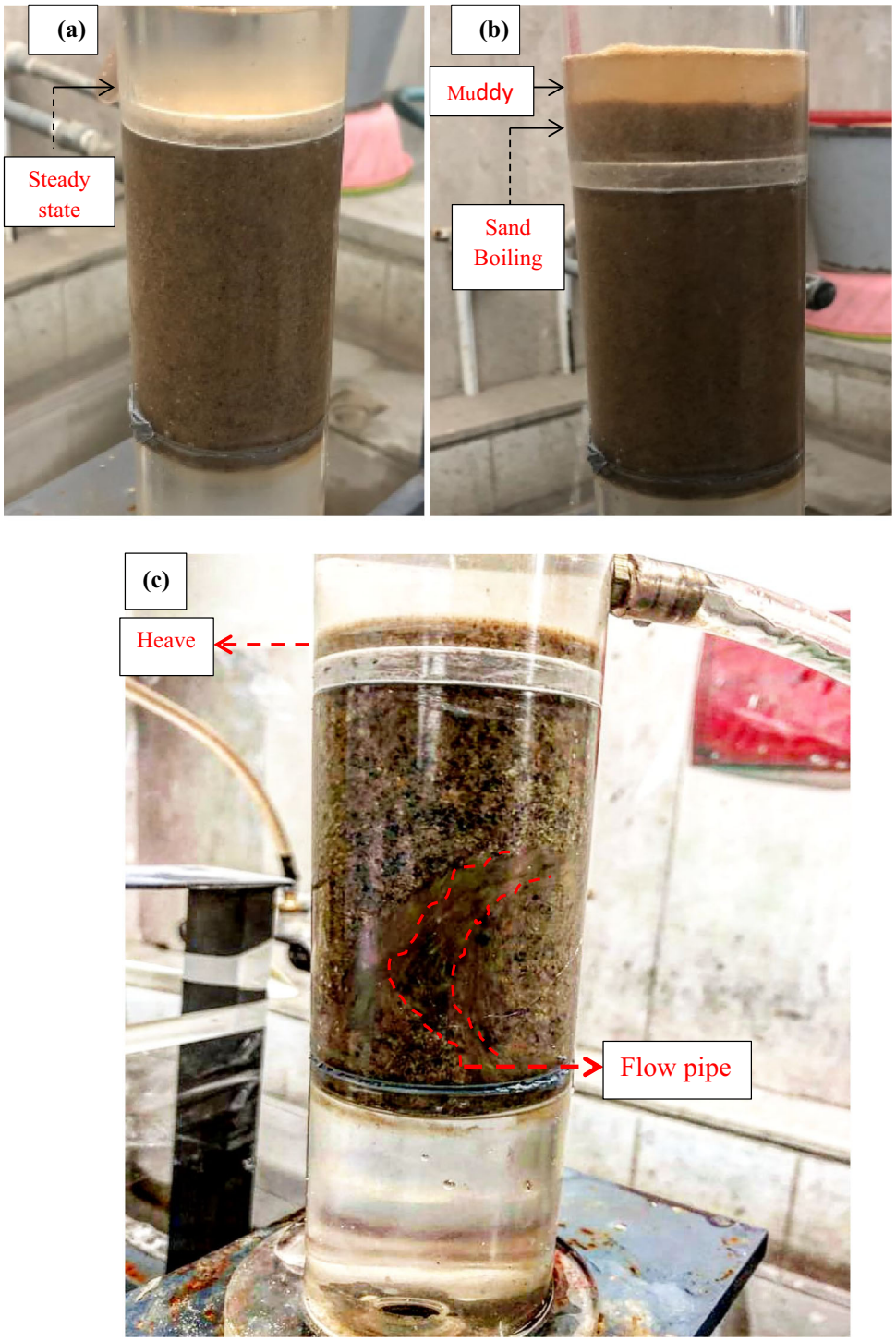

Fig. 8 The situation of the sample in the sand boiling test: **a** $i \leq i_{cr}$, **b** $i > i_{cr}$ and **c** moment of starting sand boiling phenomenon

Table 4 displays the effect of variations in relative density and uniformity coefficient on soil hydraulic parameters with $C_u > 1$ such as the amount of seepage force at the boiling point, critical hydraulic gradient and permeability coefficient. It should be noted that the amounts of heave in Table 4 have been measured for the pre-boiling point. For soils 1, 2, 3 and 4 with an increase in relative density of 80%, the changes in the longitudinal strain of the samples at the time of hydraulic failure were 0.02, 0.04, 0.05 and 0.05, respectively, indicating that the denser samples at the moment of boiling occurrence have a higher strain capacity. According to the results of the soils 1 to 4, the amount of heave in samples with loose compaction is very low. However, with increasing the relative density of the specimens, the heave

Table 4 Results of sand boiling tests on the soil samples with uniformity coefficient bigger than 1

Soil type	D_r%	$\gamma_{dSample}$	n	i_{cr}	k (cm/s)	i_{cr} (*Terzaghi*)	MQ	F(N)	Heave (mm)
Soil1, Cu = 2.02	0	1.36	0.48	0.78	0.078	0.84	1.08	1.53	0
	20	1.41	0.46	0.98	0.059	0.87	0.89	1.92	0
	50	1.49	0.43	0.98	0.055	0.93	0.95	1.92	1
	80	1.59	0.39	1.50	0.030	0.99	0.66	2.94	2
Soil2, Cu = 3.38	0	1.42	0.46	1.17	0.296	0.88	0.75	2.29	0
	20	1.48	0.43	1.18	0.167	0.92	0.78	2.31	0
	50	1.59	0.39	1.37	0.129	0.99	0.72	2.68	1
	80	1.71	0.35	1.89	0.063	1.06	0.56	3.71	4
Soil3, Cu = 4.46	0	1.46	0.44	1.18	0.352	0.90	0.76	2.31	0
	20	1.52	0.42	1.18	0.174	0.94	0.80	2.31	1
	50	1.62	0.38	1.43	0.120	1.00	0.70	2.80	2
	80	1.73	0.34	1.93	0.059	1.07	0.55	3.78	5
Soil4, Cu = 6.21	0	1.48	0.44	1.21	0.167	0.92	0.76	2.37	2
	20	1.54	0.41	1.51	0.128	0.95	0.63	2.96	2
	50	1.64	0.38	1.56	0.118	1.02	0.65	3.06	4
	80	1.75	0.33	2.30	0.058	1.08	0.47	4.51	7

Table 5 Results of sand boiling tests on the reinforced samples by geotextile

C_u	Type of sample	Geotextile texture	i_{cr}	k(cm/s)	F(N)
	Unreinforced	–	1.50	0.030	2.94
	One layer	Non-woven	1.78	0.029	3.49
Soil1, $C_u = 2.02$	One layer	Woven	2.14	0.026	4.19
	Two layers	Non-woven	2.27	0.029	4.45
	Two layers	Woven	2.67	0.021	5.23
	Unreinforced	–	1.89	0.063	3.71
	One layer	Non-woven	2.33	0.058	4.57
Soil2, $C_u = 3.38$	One layer	Woven	2.43	0.047	4.76
	Two layers	Non-woven	2.89	0.045	5.67
	Two layers	Woven	3.12	0.031	6.12
	Unreinforced	–	1.93	0.059	3.78
	One layer	Non-woven	2.23	0.058	4.37
Soil3, $C_u = 4.46$	One layer	Woven	2.41	0.057	4.72
	Two layers	Non-woven	2.77	0.041	5.43
	Two layers	Woven	3.38	0.034	6.63
	Unreinforced	–	2.30	0.058	4.51
	One layer	Non-woven	2.84	0.058	5.57
Soil4 $C_u = 6.21$	One layer	Woven	2.87	0.045	5.63
	Two layers	Non-woven	3.42	0.045	6.71
	Two layers	Woven	3.76	0.035	7.37

values have been enlarged and the specimens tolerated more longitudinal strain against boiling. In addition to the compaction condition of the samples, the uniformity coefficient value affects the deformation of the samples. Based on the results in Table 4, with increasing the uniformity coefficient by 4.19 at relative densities of 0, 20, 50 and 80%, the amount of variations in the heave becomes 2, 2, 3 and 5 mm, accordingly, which illustrates that with increasing relative density, the rate of heave has risen with more intensity against changes in the uniformity coefficient. It can be concluded that soils with non-uniformity granulation revealed more deformation at the critical hydraulic gradient point. As it can be seen, the deformation value of soil 4 (with a uniformity coefficient of 6.21) at a relative density of 80% has been 7 mm, while this amount (heave) for soil 1 in the same compaction condition is 2 mm.

Table 6 Results of sand boiling tests on the soil samples with $C_u = 1(Dr = 0)$

Soil type	i_{cr}	k(cm/s)	F(N)	i_{cr} (*Terzaghi*)	MQ
Soil5	Not exist	Re > 1	–	0.85	–
Soil6	Not exist	Re > 1	–	0.83	–
Soil7	4.2	Re > 1	8.24	0.80	–
Soil8	2.95	Re > 1	5.78	0.81	–
Soil9	1.8	Re > 1	3.53	0.80	–
Soil10	1.2	Re > 1	2.35	0.76	0.64
Soil11	0.91	0.3319	1.78	0.77	0.85
Soil12	0.84	0.1771	1.64	0.77	0.92
Soil13	0.78	0.0528	1.53	0.76	0.97
Soil14	0.67	0.0286	1.31	0.75	1.12

Table 5 presents the results of sand boiling tests on the reinforced samples by geotextile which indicates that samples with a uniformity coefficient greater than 1 in dense conditions have been improved by geotextiles against boiling. Based on the results, it is observed that the reinforced sample has better control in water seepage and increasing the number of geotextile layers improves the resistance of sandy soil against hydraulic failure. It should be noted that the type of geotextile also affected the test results. So that with reinforcing soil 1, 2, 3 and 4 by woven geotextile in two layers, the permeability coefficient decreased by 30, 50, 42.3 and 39.6%, respectively. In fact, geotextiles have an effective role in controlling seepage from the device. Similar results are also obtained and presented in Table 5 for reinforced samples by non-woven geotextiles.

The results permeability coefficient, seepage force and critical hydraulic gradients of the particle diameter of completely uniform samples ($C_u = 1$) are summarized in Table 6. According to the results of the performed experiments on soils 7 to 14, it can be suggested that by increasing the diameter of sand particles by 2.18 mm, the required water head for sand boiling in the upstream area becomes 35.3 cm. Soils 5 and 6 with a diameter of 4.75 and 3.35 mm, respectively, resisted upstream hydraulic pressures and no signs of boiling were observed on the downstream soil surfaces. For soils 5 and 6, boiling didn't occur and for soils 7, 8 and 9, despite the occurrence of boiling, the breakage point didn't appear in the velocity diagram in terms of their hydraulic gradient. Worth mentioning that the reported i_{cr} for these soils belong to a point at which upward soil particles movement has been seen.

The values of Reynolds number for soils 5 to 10 in all heights of the reservoir water table were more than 1, so the permeability coefficient hasn't been calculated for these samples. In other words, in samples 5 to 10 ($D \geq 1$ (mm)), there is no linear relationship could not be obtained between flow velocity and hydraulic gradient. However, by decreasing the particle diameter in samples 11 to 14 ($D < 1$ (mm)), Due to the reduction of flow rate and the existence of laminar flow, the Reynolds number of the flow is less than 1 and the permeability coefficient has been calculated for these samples.

Furthermore, in Tables 4 and 6, a comparison between the theoretical relationship of Terzaghi [11] and experimental test results has been conducted. In this comparison, in addition to soils 5 and 6, soils 7, 8 and 9 due to the lack of breakage of the flow velocity diagram in terms of hydraulic gradients, were not included. In this comparison, the Model Quality (MQ) statistical index has been used, which represents the ratio of the calculated critical hydraulic gradient through the theoretical relationship (i_{crt}) to the experimental critical hydraulic gradient (i_{crm}) results (Eq. 9).

$$\mathrm{MQ} = \frac{i_{\mathrm{cr\ t}}}{i_{\mathrm{cr\ m}}} \tag{9}$$

By calculating the model quality index for all samples, the mean and variation coefficient of the MQ statistical population for this comparison are 0.77 and 21%, respectively. If this index becomes 1, it indicates that the relationship of Terzaghi [11] had high validity for predicting the critical hydraulic gradient of soil. For example, the MQ index for soils 1 and 2 at loose conditions is 1.08 and 0.75, accordingly. Based on the results presented in Tables 4 and 6, the Terzaghi model has the best and worst predictions for the critical hydraulic gradient of soil 13 ($\mathrm{MQ}_{\mathrm{soil13}} = 0.976$) at the loose condition and soil 4 ($\mathrm{MQ}_{\mathrm{soil4}} = 0.473$) at a dense condition, correspondingly. In general, the proposed equation by Terzaghi [11] for i_{cr}, predicts hydraulic gradients of uniform soils in loose condition with high accuracy, but on the other hand, the calculation of critical hydraulic gradients using this model for well-graded soils at high relative densities due to the high error of this model is not recommended. Figure 9 shows the experimental and calculated results using Terzaghi's relationship.

It can also be seen in Fig. 9 that soils that had a high resistance to boiling are far from the same function and show that the Terzaghi relationship has a low value in determining the hydraulic gradient of these soils. In other words, for loose and poorly graded samples where sand boiling has occurred in the lower gradient (less than 1.1(zone A)), the Terzaghi model has high validity and has the points of maximum compliance with the line (same function).

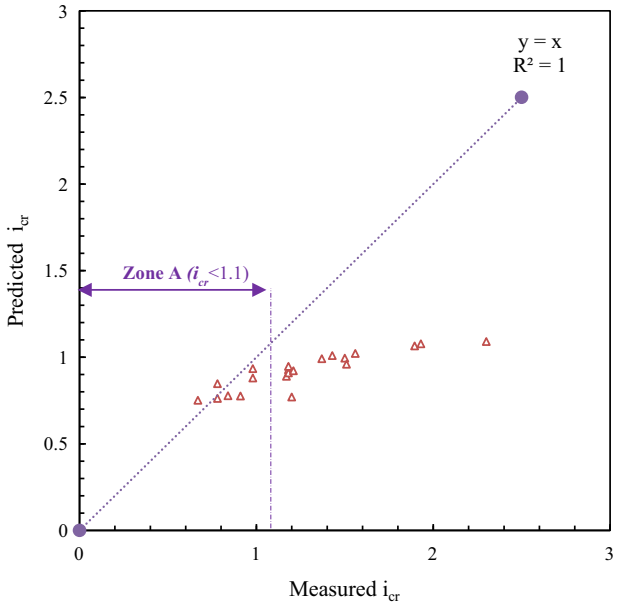

Fig. 9 Predicted vs measured critical hydraulic gradients

5.1 The Effect of the Relative Density of the Sample (for $C_u > 1$)

According to Fig. 10, for soils 1 to 4 ($C_{u>}$ 1), with rising relative density, the trend of critical hydraulic gradient variations is ascending and the samples have been improved. In fact, as the relative density of the sample increases, the breaking point of the graph (v-i) is shifted to the right, as a result of a sudden increase in flow velocity occurs at a point with a higher hydraulic gradient. In addition, the slope of the graphs before the breaking point ($i < i_{cr}$) decreases with increasing the relative density (i.e. decreasing the permeability of the samples), for instance, the values of seepage force and hydraulic gradient for the hydraulic failure of soil 1 with 80% increase in relative density (i.e. dense sample) have increased by about 100% and also the permeability coefficient of this sample has changed from 0.078 to 0.03 cm /s.

Figures 11 and 12 display that relative density changes have affected the critical hydraulic gradient and seepage force for soils 1 to 4. As it can be seen, soil 4 at relative densities of 0 and 80%, reached the critical hydraulic gradient of 1.21 and 2.3, respectively, and also, the seepage force has increased by 90%. This type of variation of critical hydraulic gradient and hydraulic conductivity has also been reported by other researchers. Ren et al. [32], Terzaghi [11] and Zhou et al. [14] investigations show porosity (relative density) has a significant effect on these hydraulic parameters (i_{cr}, k & F).

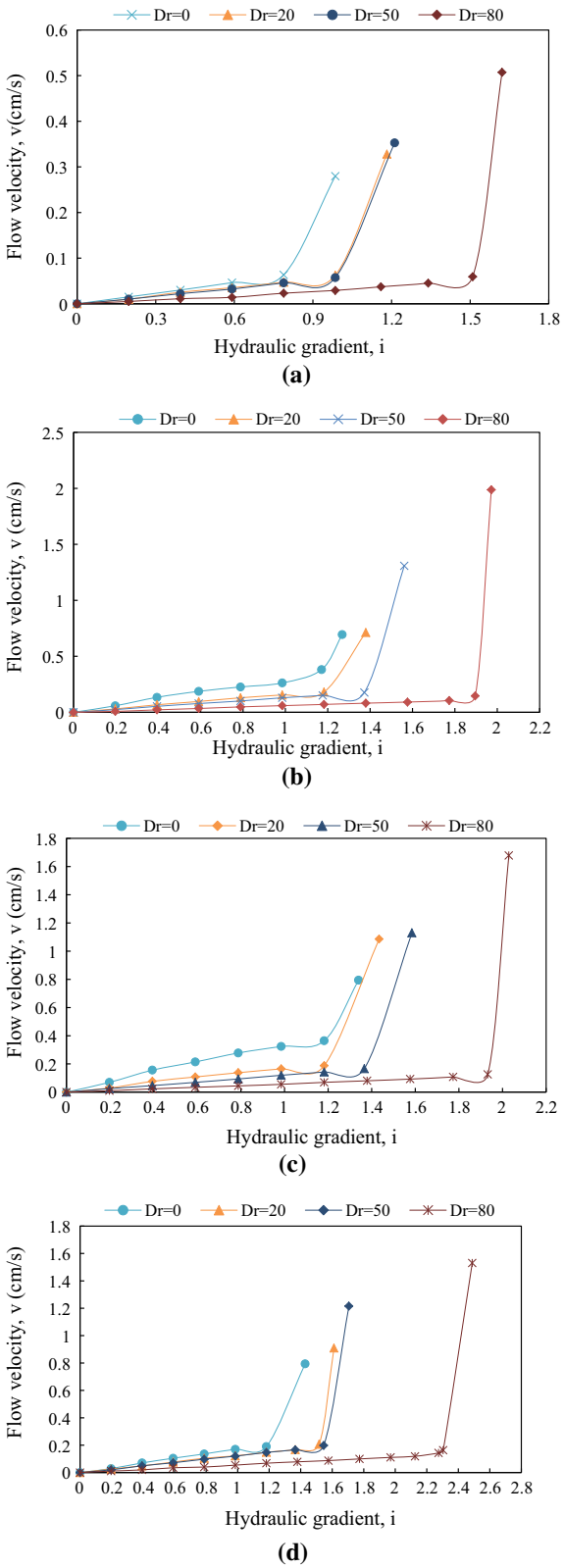

Fig. 10 Flow velocity against hydraulic gradient for different relative density: **a** $C_u = 2.02$, **b** $C_u = 3.38$, **c** $C_u = 4.46$ and **d** $C_u = 6.21$

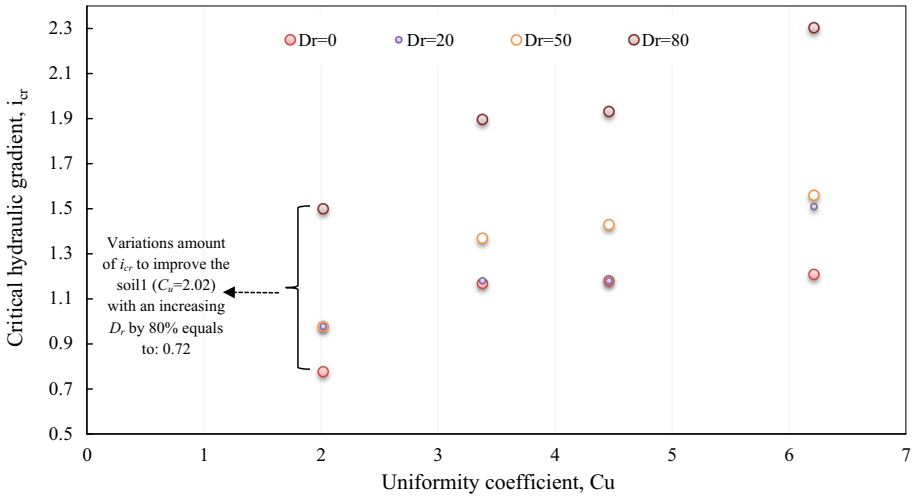

Fig. 11 Amounts of the critical hydraulic gradient versus relative density for different uniformity coefficient

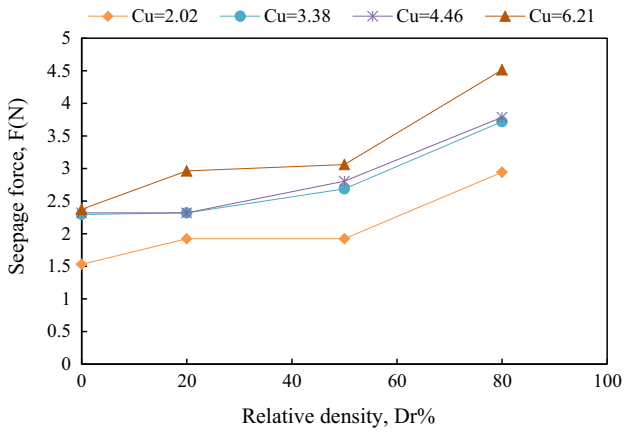

Fig. 12 Amounts of seepage force versus relative density for different uniformity coefficient

5.2 Effect of Uniformity Coefficient ($C_u > 1$)

The effect of the uniformity coefficient on the values of the hydraulic gradient and the seepage force at the moment of boiling are shown in Figs. 13 and 14, accordingly. Based on the results, for soils 1 to 4 in different compaction conditions, it can be concluded that at a constant relative density, the amount of critical hydraulic gradient increases with an increasing uniformity coefficient of samples and the samples with non-uniformity granulation indicate more resistance against the boiling. At a relative density of 80%, the value of seepage force for boiling related to soils 1 and 4 becomes 2.94 and 4.51 (N), respectively. By improving soil granulation, more hydrodynamic force is required for heave failure. Igwo et al. [33] performed a series of experiments to determine the maximum shear stress on loose sands with different uniformity coefficients and found out that sandy soil with high uniformity coefficient tolerates higher shear stress and

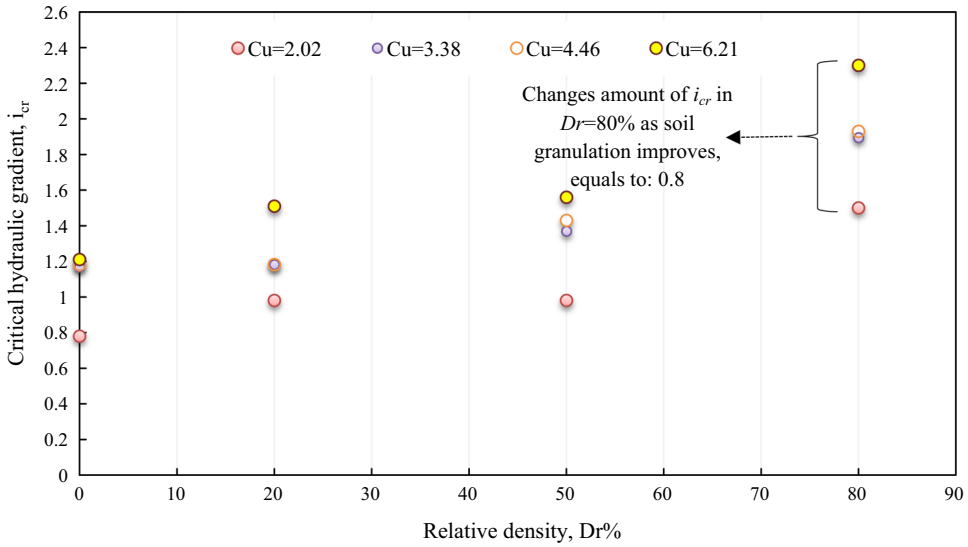

Fig. 13 Amounts of the critical hydraulic gradient versus uniformity coefficient for different relative density

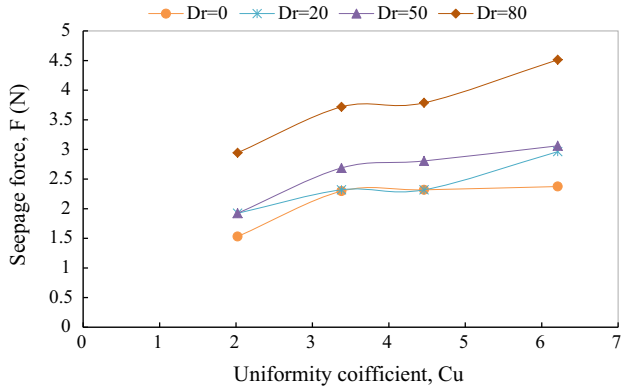

Fig. 14 Amounts of seepage force versus uniformity coefficient for different relative density

also the peak shear stress has a direct relation with soil uniformity coefficient. Therefore, it can be concluded that growing the uniformity coefficient increases the shear strength and weight of the sample, as results in upward water seepage, more hydraulic gradient is required for boil in well-graded sand.

It can be seen in Fig. 13 that the value of the critical hydraulic gradient at a relative density of 80% for soils 1 and 4 is 1.5 and 2.3, correspondingly. In fact, for sand with a specific gravity of 2.65 and a relative density of 80% with a change in uniformity coefficient from 2.02 to 6.21, the critical hydraulic gradient has increased by 53%. This increasing trend of resistance is also observed in relative densities of 0, 20 and 50%.

5.3 Effect of Geotextiles on Dense Sands with $C_u > 1$

Figure 15 shows the changes in flow velocity against the hydraulic gradient in upward water seepage for soils 1 to 4 at a relative density of 80% in reinforced and natural samples. The results indicate that by adding geotextiles to the sandy soil, the boiling of the sand is delayed and the reinforced sands show more resistance to water seepage. For example, in soil 3 with $C_u = 4.46$, by adding two layers of woven geotextiles, the critical hydraulic gradient is increased by 1.45.

Figures 16 and 17 represent the effect of the type and number of layers of geotextile on the required seepage force for boiling and the permeability coefficient of samples 1 to 4. According to the histogram of seepage force and chart of permeability coefficient, it can be concluded that woven geotextile has a greater impact on soil improvement than non-woven geotextile and water seepage rate is lower in these samples. In addition, the measured seepage force at the boiling moment is higher for woven geotextiles. Furthermore, the use of two layers of reinforcement increases the resistance of the sample to boiling rather than one layer. For instance, in soil 4($C_u = 6.21$), it is observed that in reinforcement with non-woven geotextile, the seepage force in single and double layers is 5.57 N and 6.71 N, respectively, while by replacing the woven geotextile, the seepage force changes to 5.63 N and 7.379 N, correspondingly.

Figure 18 shows the Histogram of the improvement percentage for soil 1 to 4 in dense conditions. As it can be seen, the sandy soils have been improved between 60 and 80% using geotextiles. In all samples in both single and double layer reinforcement, the highest percentage of improvement is related to woven geotextiles.

This trend of improving critical hydraulic gradient using reinforcement also considered by other researches ([15–20], and [22]). In previous studies, the soil has been improved with fibers and parameters such as length, percentage and type of fibers on the critical hydraulic gradient and permeability coefficient have been evaluated. Implementing the soil reinforcement method with randomly distributed fibers on a large scale is difficult and costly, while geotextiles can be easily applied in practice.

5.4 The Effect of Sand Particle Diameter with $C_u = 1$

Figure 19 shows the flow velocity variations against the hydraulic gradient of uniform soils (soils 5 to 14) in the loose condition. Based on the results, the break is seen only in curves of soils 10 to 14. If the diameter of the particles is greater than 1 mm, there will be no break in the diagram of (v-i). In other words, due to the high permeability of completely uniform soils with $D > 1$ mm, the flow has been turbulent before and after the hydraulic failure and a sudden difference in the amount of flow discharge doesn't occur. For particles diameters of 1 and 0.18 mm, the value of critical hydraulic gradient is 1.2 and 0.67, respectively. As a result, it can be established that boiling occurs in fine sands earlier. In addition, based on the results presented in Fig. 19, the slope of the diagram (permeability coefficient) has reduced with decreasing sand diameter.

Figures 20 and 21 demonstrate the values of the hydraulic gradient and the seepage force in terms of the diameters of the particles of perfectly uniform sands in the loosest state. It can be seen in Fig. 20 that the particle diameter in uniformly sands has a significant effect on the critical hydraulic gradient. Moreover, in accordance with Fig. 21, the regression equation passing through the diagram of seepage force versus particles diameter with a correlation coefficient of 0.96 is equal to $F = 2.86D + 0.69$. Based on this relationship, by increasing the diameter of the particles (mm), the seepage force (N) for boiling the specimens is changed at a positive rate of 2.86(N/mm). This increase in strength is due to the increase in the internal friction of particles in coarse sand against the fine sand.

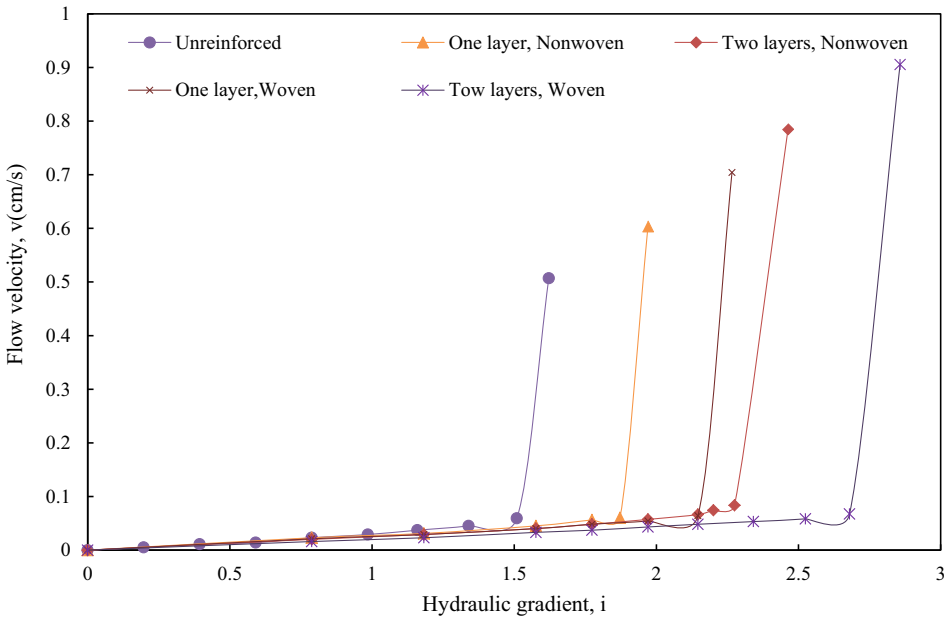

(a)

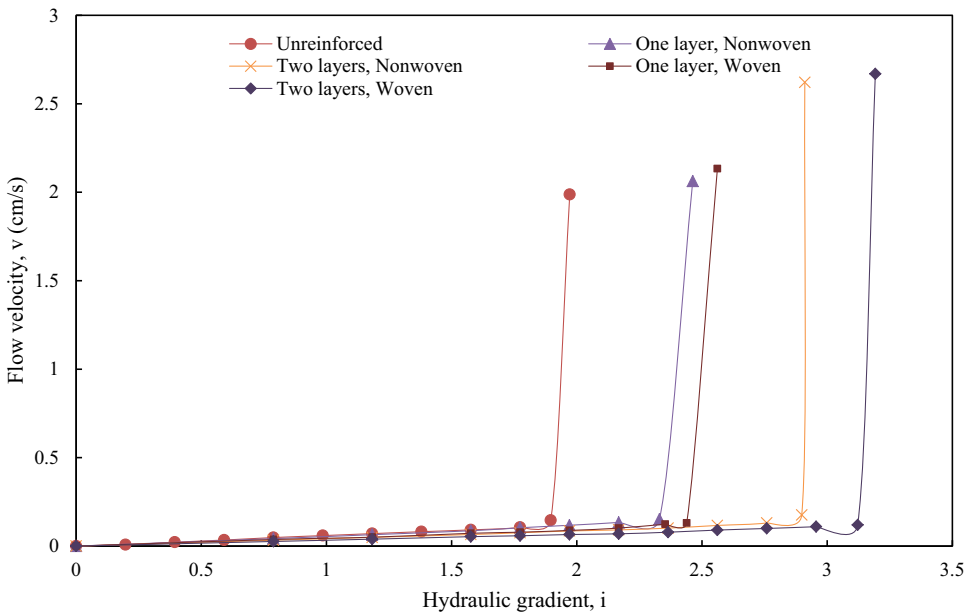

(b)

Fig. 15 Flow velocity against hydraulic gradient for reinforced samples: **a** $C_u = 2.02$, **b** $C_u = 3.38$, **c** $C_u = 4.46$ and **d** $C_u = 6.21$

Zhou et al. [14] by conducting a theoretical and laboratory study, presented the chart of the hydraulic gradient in terms of a mean diameter of the grains and found that with increasing the average diameter of the soil particles, more hydraulic gradient is required for piping occurrence. Kara et al. [34] also performed direct shear experiments on uniformly sand samples with different diameters and concluded that the internal friction angle of uniform sand materials surges with increasing particles diameter. Accordingly, coarse sand due to an increase in resisting shear stress can bear higher hydraulic gradients in upward water seepage.

5.5 Multivariate Linear and Nonlinear Regression Models

Obtained data and information from experiments in various fields can be modeled using mathematical and statistical analysis to determine the relationship between variables. In fact, to save time and costs and by using mathematical and statistical modeling that apply to the results of various experiments, prediction can be presented for an event that does not require accomplishing the test anymore. Linear and nonlinear regression methods are mathematical algorithms based on statistical reasoning that are proposed to predict data's trend.

Fig. 15 continued

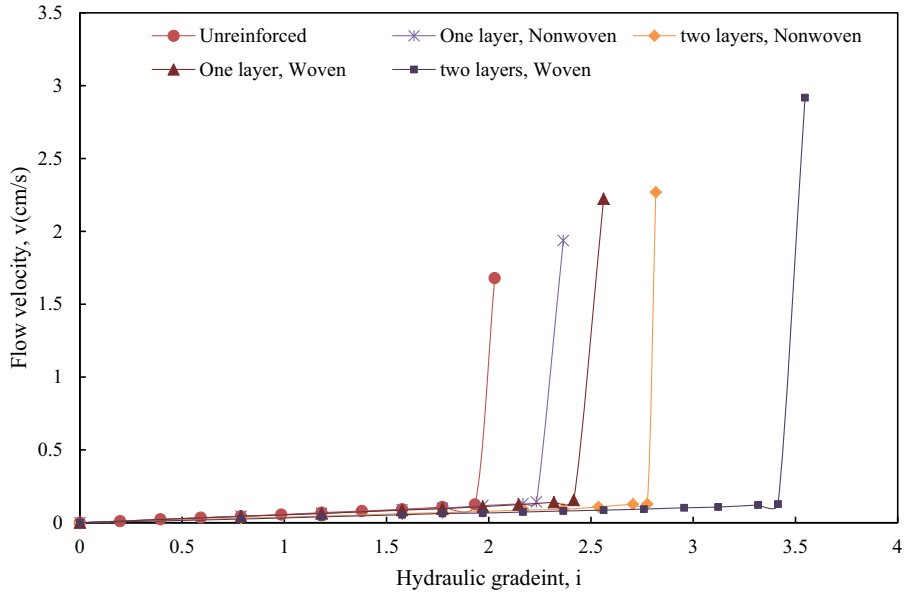

(c)

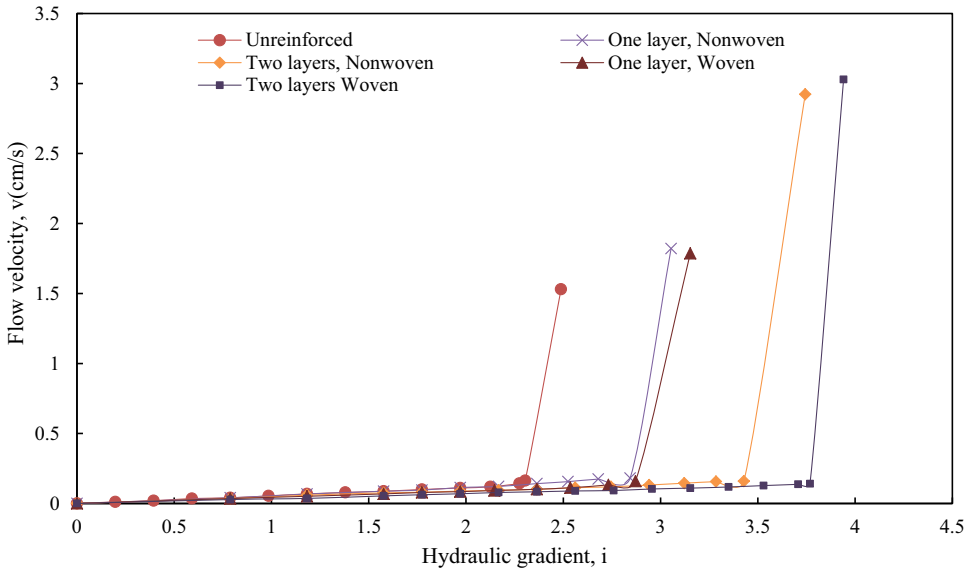

(d)

In this study, Multivariate Linear and Nonlinear Regression (MLR & MNLR) have been presented to determine the relationship between independent parameters such as uniformity coefficient and relative density with the dependent variable of seepage force which has been applied to the experimental test results with a uniformity coefficient greater than 1 (i.e. soils 1, 2, 3 and 4). This regression model has two properties (independent variable) of $x_1 = C_u$ and $x_2 = D_r\%$ and a hypothesis function (dependent variable) $y = F\ (C_u,\ D_r)$ to forecast the seepage force. In each prediction model, a hypothesis function exists that represents the behavior of the variables with each other. In these functions, there are constant coefficients that are considered unknown. Degree of freedom is a factor that determines the validity and certainty of regression, which is equal to the difference between the number of observational data and the number of the constant parameters of the hypothesis function. In this study, by examining the outcomes of sand boiling experiments on soil 1 to 4, the number of seepage force data becomes 16 for two hypotheses functions are presented in the form of Eqs. 10 and 11.

$$y = \beta_0 + \beta_1 x_1 + \beta_2 x_2 \tag{10}$$

$$y = \beta_0 + \beta_1 x_1^2 + \beta_2 x_2^2 + \beta_3 x_1 + \beta_4 x_2 + \beta_5 x_1 x_2 \tag{11}$$

Equations 10 and 11 are linear and parabolic hypothesis functions, respectively. β_j are constant coefficients of these

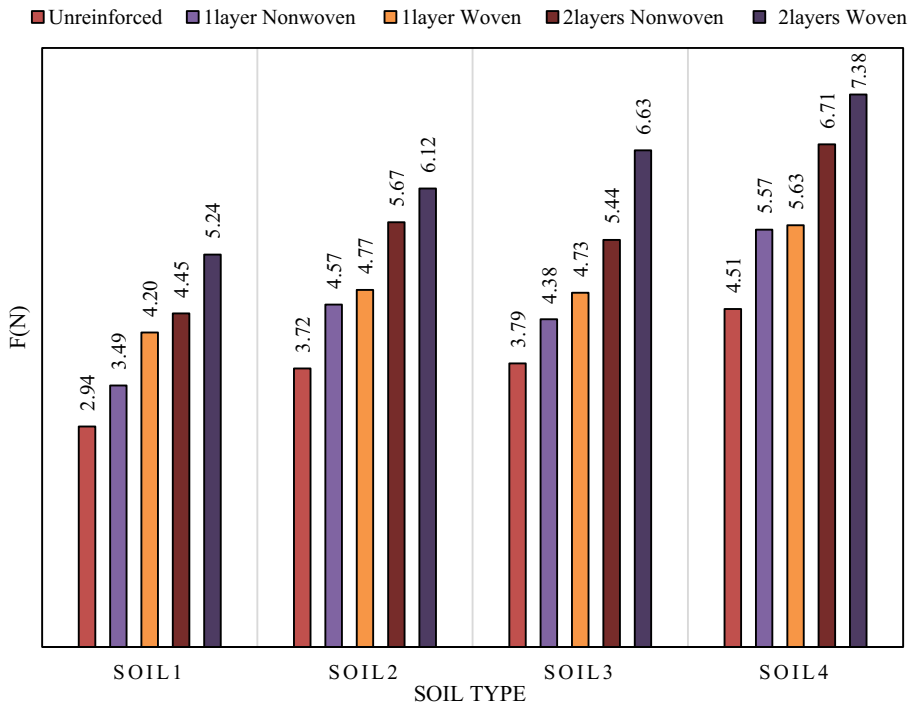

Fig. 16 Amount of seepage force at the boiling time for reinforced samples by woven and non-woven geotextile in one and two layers modes

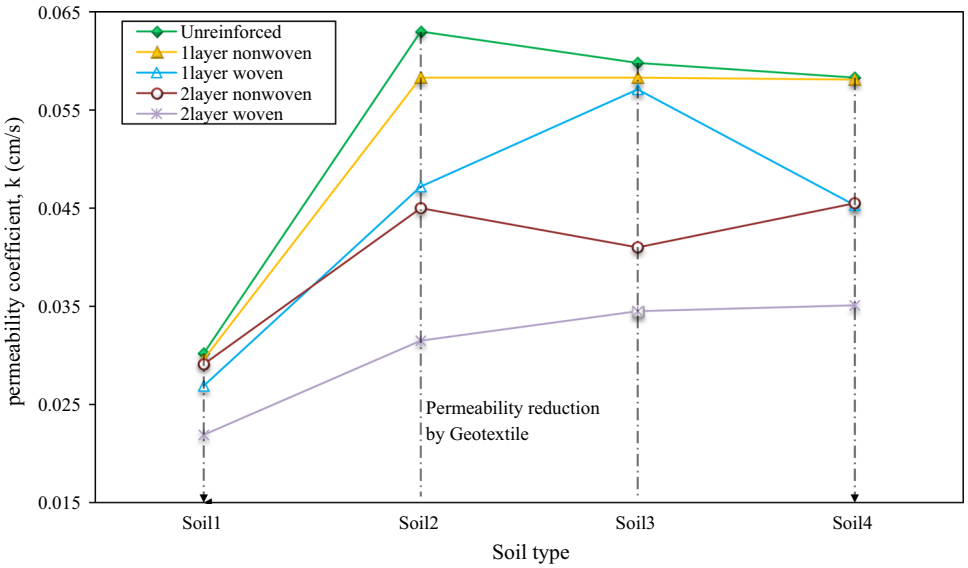

Fig. 17 Variations of permeability coefficient for reinforced samples by woven and non-woven geotextile in one and two layers modes

functions. In this study, the degree of freedom for linear and nonlinear regression is 13 and 10, correspondingly. In regression models, to obtain constant coefficients, the classic method of the least square of Errors [35] is used to produce the most conformed model. If Y_i and y_i show the amount of observational data and the prediction value of the hypothesis function for the ith test, accordingly, then the sum of the square of the error (Δ^2) will be achieved from Eq. (12):

$$\Delta^2 = \sum_{i}^{n} (Y_{\mathrm{i}} - y_{\mathrm{i}})^2 \tag{12}$$

In Eq. (12), n is the number of data. To obtain the model with the most conformity, the derivative of Δ^2 with respect to β_{j} must be considered zero (optimization):

$$\forall j, \frac{d\Delta^2}{d\beta_{\mathrm{j}}} = 0 \tag{13}$$

According to Eq. (13), for each constant coefficient (regression unknowns), an equation is generated that by solving this collection of equations, the most accurate model to predict the data is achieved.

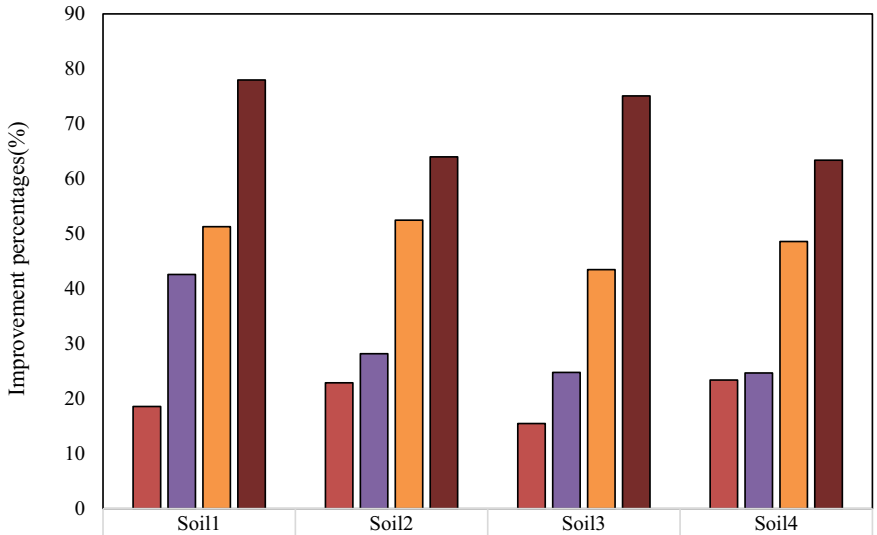

	Soil1	Soil2	Soil3	Soil4
1 layer Nonwoven	18.6	22.9	15.5	23.4
1 layer Woven	42.6	28.2	24.8	24.7
2 layers Nonwoven	51.3	52.5	43.5	48.6
2 layers Woven	78	64	75.1	63.4

Fig. 18 Amount of improvement percentage for reinforced samples by woven and non-woven geotextile in one and two layers modes (Improvement percentage (%) = $(i_{cr(\text{reinforced})} - i_{cr(\text{unreinforced})} / i_{cr(\text{unreinforced})}) * 100$)

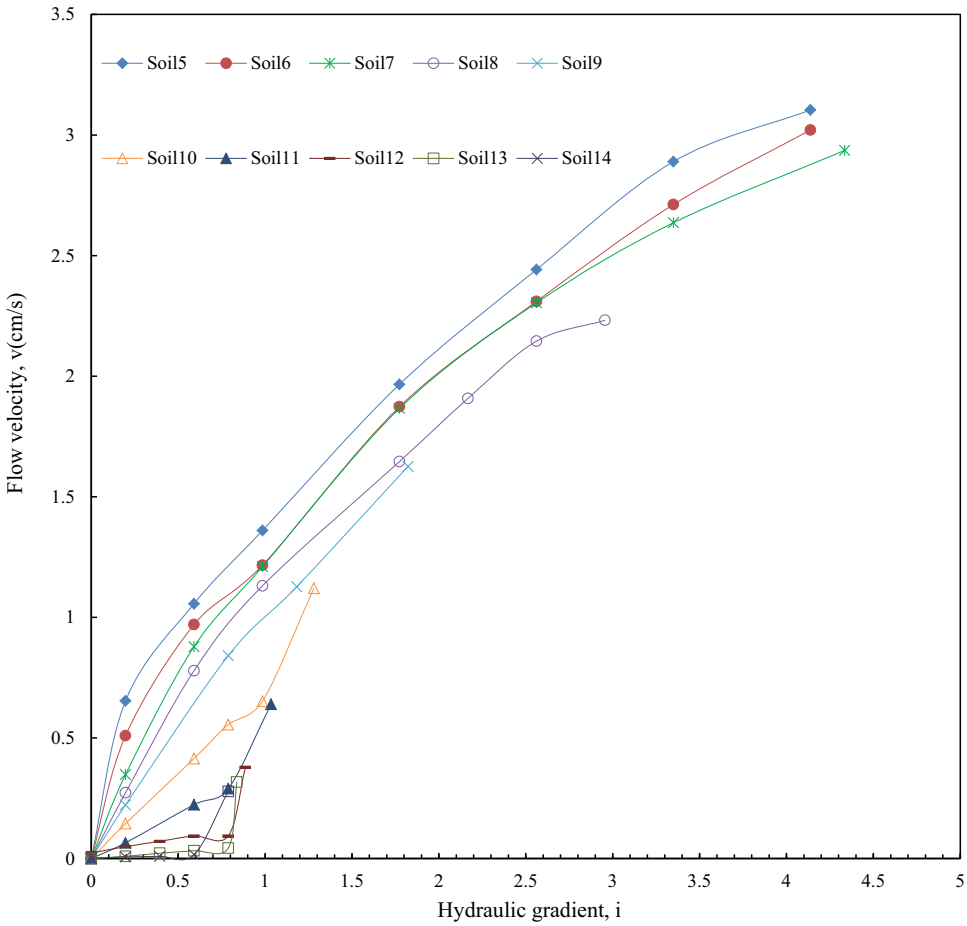

Fig. 19 Variations of flow velocity against hydraulic gradient for soils with $C_u = 1$

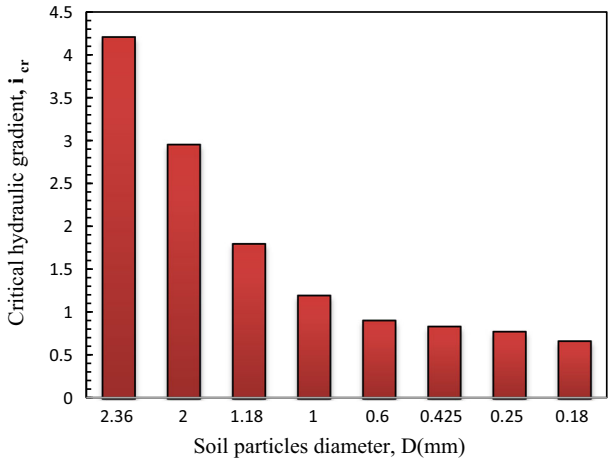

Fig. 20 Critical hydraulic variation versus particles diameter ($C_u = 1$)

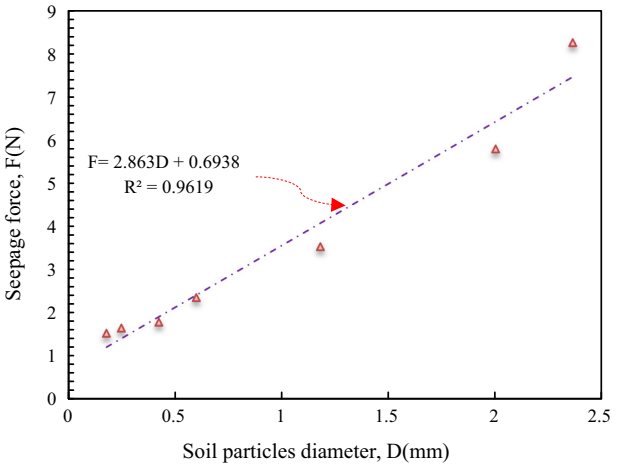

Fig. 21 Seepage force versus particles diameter ($C_u = 1$)

Thereafter, 2 characteristics of R^2 and RMSE are calculated for the regression model. R^2 is the determination coefficient of the model. As this coefficient gets closer to 1, a higher percentage from dependent data has been determined via the independent features. RMSE is the root-mean-square errors of the predicted and observed data, Also, as this value gets closer to zero, the presented regression model has less error. These two characteristics are calculated based on Eqs. (14 and 15).

$$R^2 = \frac{\left(\sum_i^n (y_i - y_{ave})(Y_i - Y_{ave})\right)^2}{\sum_i^n (Y_i - Y_{ave}) \sum_i^n (y_i - y_{ave})} \tag{14}$$

$$\text{RMSE} = \sqrt[2]{\sum_i^n \frac{(y_i - Y_i)^2}{n}} \tag{15}$$

where Y_{ave} and y_{ave} are the averages of the predicted and measured data, respectively. In this study, the outcome of linear and nonlinear regression analysis of 2 variables (uniformity coefficient and relative density) on the required seepage force for the hydraulic failure of the samples have been shown in Table 7:

Table 7 Results of regression models

Regression type	R^2	RMSE
MLR	0.93	0.279(N)
MNLR	0.97	0.162(N)

$$F(N) = 0.97255 + 0.25626C_u + 0.0191D_r(\text{MLR}) \tag{16}$$

$$\begin{aligned} F(N) = {} & 0.858511 - 0.040637C_u^2 + 0.000272D_r^2 \\ & + 0.519167C_u - 0.010823D_r \\ & + 0.00198C_uD_r\,(\text{MNLR}) \end{aligned} \tag{17}$$

Equations (16 and 17) show the linear and nonlinear regressions passing through the experimental data. Based on Eq. (16), the coefficients of C_u and D_r are greater than zero. It can be concluded that with increasing the uniformity coefficient and relative density, the amount of seepage force increases and the sample is improved. It should be noted that in Eqs. (16 and 17), relative density values are entered in the form of the percentage. As well as the values of determination coefficient (R^2) for nonlinear (parabolic) regression are higher than linear regression that indicates, more data has been determined by the parabolic model. Whilst, the root-mean-square errors (RMSE) of the linear model is about 0.12 N higher than the parabolic model. Figure 22 displays the graphs of the predicted data in terms of measured data for both linear and nonlinear regression models. In this Figure, it can be seen clearly that the points for the linear model have more dispersion toward the identity function (y = x) and in the nonlinear regression diagram, the matching of the points on the identity function seems more. Generally, it can be said, nonlinear regression is more accurate than linear regression.

6 Conclusion

In this paper, while designing and fabricating a device to simulate the sand boiling phenomenon, experimental and statistical studies have been implemented on different types of sandy soils. The effects of gradation characteristics uniformity coefficient and soil particle diameter, relative density, type and layers number of geotextile on sand hydraulic parameters such as seepage force, critical hydraulic gradient and permeability coefficient have been investigated. Furthermore, linear and nonlinear regression models are presented. The main results of this research are as follows:

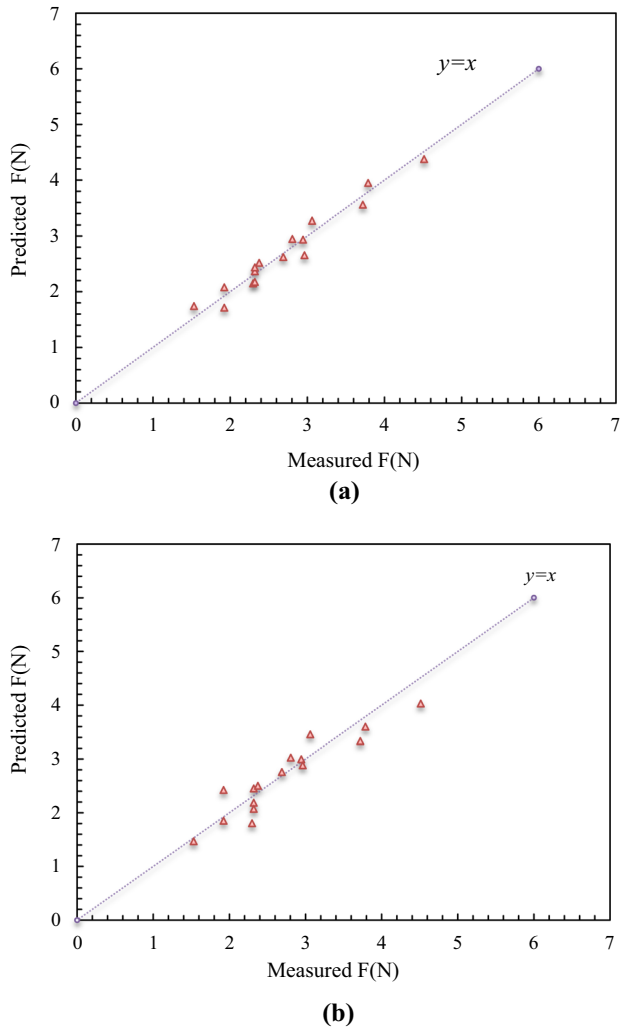

Fig. 22 Variations of predicted against measured seepage force during sand boiling: **A** MNLR, **B** MLR

1. With an increase in the uniformity coefficient, the trend of the changes in maximum and minimum dry unit weight of sandy soils is ascending. In this study, the maximum dry density for sands with uniformity coefficients of 2.02, 3.38, 4.46 and 6.21 are 1.67, 1.8, 1.82 and 1.84 g/cm^3, respectively. The maximum void ratio for soil 5 with a diameter of 4.75 mm and soil 14 with a diameter of 180 μm is 0.96 and 1.22, correspondingly, which indicates that coarser sands have less porosity.
2. In sandy soils with a uniformity coefficient greater than 1 with increasing compaction and relative density, hydraulic failure occurs at higher hydraulic gradients. For instance, with an 80% increase in relative density, the resistance against boiling increased by 100% for a soil with a uniformity coefficient of 2.02. On the other hand, at constant relative density, the critical hydraulic gradient of the soil has increased with the improvement of gradation characteristics (increasing uniformity coefficient), and well-graded samples indicated more resistance to hydraulic failure. As an example, the critical hydraulic gradient of soil 1 with Cu = 2.02 and soil 4 with Cu = 6.21 in dense conditions are 1.5 and 2.3, accordingly.
3. In the reinforcement by geotextile, the reinforced specimens have more resistance than the natural specimen, which can be attributed to the reduction of the permeability coefficient in the reinforced specimens. In addition, samples reinforced with 2 layers of geotextile failed at higher hydraulic gradients. Also Woven geotextiles due to lower water permeability have better performance in the improvement process. The average percentage of improvement with woven and non-woven geotextiles for two-layer mode is 70% and 49%, respectively.
4. For soils in the loosest compaction condition with C_u = 1, the diameter of sand particles (D) has significantly affected the hydraulic parameters of the sample. By considering the flow velocity diagram with respect to the hydraulic gradient for soils with particles diameter greater than 1 mm, there is no maximum point (breakage) that cannot be observed and therefore the critical hydraulic gradient for these samples cannot be calculated. Furthermore, reducing the diameter of the particles in perfectly uniform soils decreases the permeability coefficient and critical hydraulic gradient.
5. Two linear and non-linear regression models have been presented to predict the required seepage force for hydraulic rupture of sands with a uniformity coefficient greater than 1. These models indicate the effect of relative density and uniformity coefficient on the occurrence of sand boiling. In the linear model, the coefficients of the independent variables of the regression are positive, so it can be concluded that with increasing the relative density and uniformity coefficient, the resistance of the sample to hydraulic failure increases. Also, the nonlinear model has a higher determination coefficient and a lower error rate than the linear model. It can be concluded that nonlinear regression has predicted the obtained data in this study with higher accuracy.
6. A laboratory study in this study shows that parameters such as uniformity coefficient, grain diameter and relative density of sandy soils are very effective on the occurrence of sand boiling phenomenon and improves the hydraulic parameters of sandy soils by adding woven and non-woven geotextiles. Using the finding of this research, it is possible to use geotextiles to increase the critical hydraulic gradient downstream of levees, dams and embankments and to avoid the risk of consequences related to the failure of these types of hydraulic structures.

This research did not receive any specific grant from funding agencies in the public, commercial, or not-for-profit sectors.

Acknowledgements The authors also thank Marayam Hojabri and Aria Maleki for their valuable technical assistance.

Funding Not applicable.

Available data and materials The obtained data from experiments are in the result and discussion section, if you need the details of laboratory results, we can send an excel file.

Code availability Not applicable.

Declarations

Conflict of interest Not applicable.

References

1. MSD.: Stability of embankments at German in waterway, issue 2011-BAW code of practice. ISSN 2192–9807, published by Bundesanstalt Fur wasserbau Karlsruhe (2011)
2. Budhu, M.: Soil mechanics and foundations. Wiley, NY (2020)
3. Tian, D.; Xie, Q.; Fu, X.; Zhang, J.: Experimental study on the effect of fine contents on internal erosion in natural soil deposits. Bull. Eng. Geol. Env. **79**, 4135–4150 (2020)
4. Vakili, A.H.; Bin Selamat, M.R.; Mohajeri, P.; Moayedi, H.: A critical review on filter design criteria for dispersive base soils. Geotechn. Geol. Eng. **36**(4), 1933–1951 (2018)
5. Jewel, A.; Fujisawa, K.; Murakami, A.: Effect of seepage flow on incipient motion of sand particles in a bed subjected to surface flow. J. Hydrol. **579**, 124178 (2019)
6. Belkhatir, M.; Schanz, T.; Arab, A.; Della, N.: Experimental study on the pore water pressure generation characteristics of saturated silty sands. Arab. J. Sci. Eng. **39**(8), 6055–6067 (2014)
7. Tao, H.; Tao, J.: Quantitative analysis of piping erosion micromechanisms with coupled CFD and DEM method. Acta Geotech. **12**(3), 573–592 (2017)
8. Peng, S.; Rice, J.D.: Inverse analysis of laboratory data and observations for evaluation of backward erosion piping process. J. Rock Mech. Geotech. Eng. **12**(5), 1080–1092 (2020)
9. Richards, K.S.; Reddy, K.R.: Experimental investigation of initiation of backward erosion piping in soils. Géotechnique **62**(10), 933–942 (2012)
10. Seed, H.B.; Duncan, J.M.: The failure of Teton dam. Eng. Geol. **24**(1–4), 173–205 (1987)
11. Terzaghi, K.: Theoretical soil mechanics, p. 11–15. Wiley, New York USA (1943)
12. Wu, L.J.: Calculation of critical hydraulic gradient for piping in cohesionless soils. Hydro-Sci. Eng. **4**, 90–95 (1980)
13. Liu, J.: Seepage stability and seepage control of soil. Water Resources and Electric Power Press, Beijing (1992).
14. Zhou, J.; Bai, Y. F.; & Yao, Z. X.: A mathematical model for determination of the critical hydraulic gradient in soil piping. In Geoenvironmental Engineering and Geotechnics: Progress in Modeling and Applications pp. 239–244, (2010)
15. Furumoto, K.; Miki, H.; Tsuneoka, N.; & Obata, T.: Model test on the piping resistance of short fiber reinforced soil and its application to river levee. In Proc., 7th Int. Conf. on Geosynthetics (pp. 1241–1244). Swets & Zeitlinger, Lisse (2002)
16. Sivakumar Babu, G.L.; Vasudevan, A.K.: seepage velocity and piping resistance of coir fiber mixed soils. J. Irrig. Drain. Eng. **134**(4), 485–492 (2008)
17. Das, A.; Jayashree, C.; Viswanadham, B.V.S.: Effect of randomly distributed geofibers on the piping behaviour of embankments constructed with fly ash as a fill material. Geotext. Geomembr. **27**(5), 341–349 (2009)
18. Das, A.; Viswanadham, B.V.S.: Experiments on the piping behavior of geofiber-reinforced soil. Geosynth. Int. **17**(4), 171–182 (2010)
19. Estabragh, A.R.; Soltannajad, K.; Javadi, A.A.: Improving piping resistance using randomly distributed fibers. Geotext. Geomembr. **42**(1), 15–24 (2014)
20. Estabragh, A.R.; Soltani, A.; Javadi, A.A.: Models for predicting the seepage velocity and seepage force in a fiber reinforced silty soil. Comput. Geotech. **75**, 174–181 (2016)
21. Yang, K.H.; Wang, J.Y.: Experiment and statistical assessment on piping failures in soils with different gradations. Mar. Georesour. Geotechnol. **35**(4), 512–527 (2017)
22. Yang, K.H.; Adilehou, W.M.; Jian, S.T.; Wei, S.B.: Hydraulic response of fibre-reinforced sand subject to seepage. Geosynth. Int. **24**(5), 491–507 (2017)
23. Langroudi, S.G.; Zad, A.; Rajabi, A.M.: Improvement of sandy soil to prevent hydraulic failure using BCF fibers and geotextiles. Arab. J. Geosci. **14**(17), 1–16 (2021)
24. ASTM Committee D-18 on Soil and Rock.: Standard practice for classification of soils for engineering purposes (unified soil classification system) 1. ASTM International (2017)
25. Das, B. M.: Soil mechanics laboratory manual (2021)
26. Skempton, A.W.; Brogan, J.M.: Experiments on piping in sandy gravels. Geotechnique **44**(3), 449–460 (1994)
27. Standard, A. S. T. M. D4254–91: Standard Test Method for Minimum Index Density and Unit Weight of Soils and Calculation of Relative Density. Annual Book of ASTM Standards, ASTM International, West Conshohocken, PA (2006)
28. Standard, A.S.T.M.: Test methods for maximum index density and unit weight of soils using a vibratory table. ASTM Standard D **4253**, 16 (2006)
29. Arvelo, A.: Effects of the soil properties on the maximum dry density obtained. (M.S.C.E.) thesis, University of Central Florida (2004)
30. Islam, M. N., Siddika, A., Hossain, M. B., Rahman, A., & Asad, M. A. (2019). Effect of particle size on the shear strength behavior of sands. arXiv preprint arXiv:1902.09079
31. Das, B.M.: Advanced soil mechanics, p. 236. CRC Press, London, UK (2019)
32. Ren, X.; Zhao, Y.; Deng, Q.; Kang, J.; Li, D.; Wang, D.: A relation of hydraulic conductivity—void ratio for soils based on Kozeny-Carman equation. Eng. Geol. **213**, 89–97 (2016)
33. Igwe, O.; Sassa, K.; Wang, F.: The influence of grading on the shear strength of loose sands in stress-controlled ring shear tests. Landslides **4**(1), 43 (2007)
34. Kara, E.M.; Meghachou, M.; Aboubekr, N.: Contribution of particles size ranges to sand friction. Eng., Technol. Appl. Sci. Res. **3**(4), 497–501 (2013)
35. Chapra, S.C.; Canale, R.P.: Numerical methods for engineers, Vol. 1221. Mcgraw-Hill, New York (2011)